

Tuning the electrical properties of the heart by differential trafficking of K_{ATP} ion channel complexes

Eric C. Arakel^{1,2,†}, Sören Brandenburg^{1,3,†}, Keita Uchida⁴, Haixia Zhang⁴, Yu-Wen Lin⁴, Tobias Kohl³, Bianca Schrul^{1,7}, Matthew S. Sulkin⁵, Igor R. Efimov⁵, Colin G. Nichols⁴, Stephan E. Lehnart^{3,6} and Blanche Schwappach^{1,2,7*}

¹Department of Molecular Biology, Center for Biochemistry and Molecular Cell Biology, Heart Research Center Göttingen, University Medicine Göttingen, Humboldtallee 23, 37073 Göttingen, Germany. Phone: +49551395961; Fax: +49551395960

²Faculty of Life Sciences, University of Manchester, Oxford Road, M13 9PT, United Kingdom.

³Department of Cardiology & Pulmonology, Heart Research Center Göttingen, University Medicine Göttingen, Robert-Koch-Straße 40, 37075 Göttingen, Germany.

⁴Department of Cell Biology and Physiology, and Center for the Investigation of Membrane Excitability Diseases, Washington University School of Medicine, 660 S. Euclid Avenue, Box 8228, St. Louis, MO 63110, USA.

⁵ Department of Biomedical Engineering, Washington University, St. Louis, MO 63110, USA.

⁶ Center for Biomedical Engineering and Technology, University of Maryland Baltimore, USA

⁷ Max-Planck Institute for Biophysical Chemistry, Göttingen, Germany

†These authors contributed equally.

*Correspondence to: blanche.schwappach@med.uni-goettingen.de

Running head: Differential Sorting of Cardiac K_{ATP}

SUMMARY

The copy number of membrane proteins at the cell surface is tightly regulated. Many ion channels and receptors present retrieval motifs to COPI and are retained in the early secretory pathway. In some cases the COPI interaction is prevented by binding of 14-3-3 proteins. However, the functional significance of this COPI/14-3-3 antagonism in terminally differentiated cells is unknown. Here we show that ATP-sensitive potassium (K_{ATP}) channels composed of Kir6.2 and SUR1 subunits are stalled in the Golgi complex of ventricular, but not atrial cardiomyocytes. Upon sustained β -adrenergic stimulation, which leads to activation of protein-kinase A (PKA), SUR1-containing channels reach the plasma membrane of ventricular cells. We show that PKA-dependent phosphorylation of the C-terminus of Kir6.2 decreases binding of COPI and thereby silences the Arg-based retrieval signal. Thus, activation of the sympathetic nervous system releases this K_{ATP} channel population from storage in the Golgi and hence may facilitate the adaptive response to metabolic challenges.

INTRODUCTION

Hormones rapidly adapt the function of cells to the physiological requirements of the organism. Regulated translocation of ion channels and transporters to the plasma membrane is one important mechanism of cellular response. Prominent examples include insulin-triggered GLUT4 translocation (Bogan, 2012) and growth-hormone-induced translocation of TRPC5 channels (Abe and Puertollano, 2011; Bezzerides et al., 2004). Specialized post-Golgi storage vesicles and endosomal membranes contribute to storage, rapid exposure and recycling of such cargo proteins but the extent of participation of the early secretory pathway in regulated deployment of membrane proteins is unknown. Here we consider metabolically sensitive ATP-sensitive potassium (K_{ATP}) channels, as an example of a heteromultimeric cargo protein that is stored in and released from the Golgi compartment upon hormone-induced signal transduction.

K_{ATP} channels are heterooctameric multimers of four pore-forming Kir6.1 or Kir6.2 subunits and four sulfonylurea receptor (SUR1 or SUR2) subunits (Nichols, 2006). Co-expression of the two subunits is necessary to achieve functional expression of K_{ATP} channels (Tucker et al., 1997) by a checkpoint mechanism (Zerangue et al., 1999): Exposure of Arg-based ER retention/retrieval motifs by Kir6.2 and SUR1 prevents cell surface transport unless stoichiometrically assembled heterooctamers are formed. Subsequent work identified COPI as the vesicle coat involved in the recognition of Arg-based signals (Michelsen et al., 2007) and 14-3-3 proteins as a cytosolic factor that facilitates efficient cell surface expression (Heusser et al., 2006). The latter finding coincided with the discovery that many ion channels and plasma membrane proteins strictly require 14-3-3 to reach the cell surface (Godde et al., 2006; O'Kelly et al., 2002; Rajan et al., 2002; Smith et al., 2011). For such cargo proteins, lack of 14-3-3 interaction leads to accumulation in the Golgi compartment (Godde et al., 2006; Zuzarte et al., 2009). Intriguingly, all cargo proteins with a 14-3-3 requirement for cell-surface expression also possess COPI-interaction motifs (Godde et al., 2006; O'Kelly et al., 2002; O'Kelly and Goldstein, 2008; Shikano et al., 2005; Smith et al., 2011; Zuzarte et al., 2009) raising the possibility that COPI/14-3-3 antagonism is a key Golgi trafficking control mechanism. 14-3-3 proteins predominantly recognize phosphorylated client proteins and participate in signal transduction cascades (Morrison, 2009). Together, these facts evoke the hypothesis

that cargo interactions with COPI and 14-3-3 might underlie physiologically regulated sorting events, in addition to providing a basic assembly checkpoint.

Native K_{ATP} channels are highly expressed in multiple tissues. In cardiac muscle cells, they couple electrical and metabolic signals at the cell surface during adaptation to stress (Zingman et al., 2002), hyperpolarizing the cells and preventing Ca^{2+} entry under conditions of energy depletion. Thus, they may offer protection from life-threatening heart damage during ischemia or sustained β -adrenergic stimulation, as demonstrated in mice with genetic deletions of K_{ATP} channel subunits (Miki et al., 2002; Suzuki et al., 2002; Yamada et al., 2006; Zingman et al., 2002). Human K_{ATP} mutations, many of which affect the trafficking of the channel (Yan et al., 2007), underlie different K_{ATP} channelopathies and can significantly increase the risk for heart disease (Nichols et al., 2013). Each K_{ATP} subunit has been identified in the heart (Philip-Couderc et al., 2008), but expression varies from region to region and can change under patho-physiological conditions (Isidoro Tavares et al., 2009; Isidoro Tavares et al., 2007; Raeis-Dauve et al., 2012). From the genetically tractable mouse heart, it is clear that SUR2A and Kir6.2 subunits are important components of ventricular K_{ATP} channels, whereas SUR1 and Kir6.2 subunits are critical for atrial channels (Flagg et al., 2008). Of note, these two subunits also form the pancreatic K_{ATP} channel complex, essential for insulin secretion and the molecular target of common antidiabetic sulfonylureas. What cellular processes control the molecular diversity of K_{ATP} channels in general, and specifically in different heart tissues such as atria and ventricles, is currently unknown. We therefore assessed K_{ATP} channel complex assembly, as well as localization and vesicular trafficking of SUR subunits in different cardiac chambers. We describe the presence of SUR1 in both chambers of the heart – calling attention to the controversial notion that sulfonylureas increase cardiovascular risk in type II diabetic patients (Garratt et al., 1999; Goldner et al., 1971; Henry, 1998).

RESULTS

Assembly status and localization of K_{ATP} channels in cardiac myocytes

We studied SUR1 and SUR2A in total membranes from dissected hearts of wild type (wt), *kcnj11*^{-/-} (Kir6.2 knockout) and *abcc8*^{-/-} (SUR1 knockout) mice (Fig. 1A; Fig. S1A). SUR1 was expressed in both atria and ventricles, but SUR2A was absent from atria (see Fig. S1B for quantification). Confocal image sections confirm scanning ion conductance microscopic observations (Korchev et al., 2000) - in ventricular myocytes SUR2A and Kir6.2 co-localize at the cell surface and at striations where T tubule membrane invaginations occur (Fig. 1B). The presence of SUR1 in ventricular myocytes (Fig. 1A) questions the concept that, in the ventricle, only SUR2A is associated with Kir6.2 (Babenko et al., 1998).

Both SURs are glycoproteins: SUR1 is N-glycosylated at positions Asn¹⁰ and Asn¹⁰⁵⁰ (Conti et al., 2002), and sites for N-glycosylation are predicted at Asn⁹ and Asn³³⁰ of SUR2. We therefore employed glycosylation analysis to characterize trafficking of these K_{ATP} channel subunits within cardiac tissue (Fig. 1C). Glycosylation of secretory and membrane proteins occurs in different compartments of the secretory pathway because the modifying enzymes are confined to the endoplasmic reticulum (ER) or different regions of the Golgi (Kornfeld and Kornfeld, 1985). Hence, N-glycosylation status, i.e. the glycans and the extent of the modification, has been used to monitor progression of such cargo proteins through the secretory pathway. Even without detailed analysis of the composition and length of the attached oligosaccharide, simple enzymatic tools can be used in combination with SDS PAGE to assess changes in electrophoretic mobility, indicative of export from the ER and passage through the Golgi. Specifically, glycans added in the ER (core glycosylation) can be removed by Endoglycosidase H (Endo H) whereas Golgi-modified (complex-glycosylated) cargo proteins are Endo H-resistant. PNGase F removes all types of N-glycosylation and can thus be used to demonstrate N-glycosylation *per se*.

In heterologous systems, cell-surface expression of SURs requires co-expression with Kir6.2 (or homologous Kir6.1) because COPI-dependent Arg-based ER-retrieval signals prevent the release of unassembled subunits from the early secretory pathway (Zerangue et al., 1999). Therefore, glycosylation status reflects not only steady-state localization of assembled complexes (duration of Golgi passage, given that the degree

of complex glycosylation is defined by the combined action of glycosyl-transferases and glycosidases in the respective compartment) but also assembly status of channel subunits (unassembled SUR remains Endo H-sensitive).

Both SURs migrate faster and hence are presumably only core-glycosylated in *kcnj11*^{-/-} hearts (Fig. 1A), suggesting that complex-glycosylation of cardiac SUR1 and ventricular SUR2A depends on co-assembly with Kir6.2. Interestingly, in wt membranes atrial and ventricular SUR1 was predominantly Endo H-resistant and hence complex-glycosylated (Fig. 1D). Concomitantly, SUR1 was Endo H-sensitive and hence only core-glycosylated in *kcnj11*^{-/-} hearts. This suggests that in the heart, Kir6.2 is the predominant assembly partner of SUR1 present in both atria and ventricles. Co-assembly of SUR1 with Kir6.2 throughout the heart was also reflected in decreased levels of cardiac Kir6.2 in *abcc8*^{-/-} mice (Fig. S1C and D). SUR1 and Kir6.2 co-assemble in the brain, and steady-state levels of either protein decrease upon knockout of the gene encoding the partner subunit (Fig. S1E). Hence decreased Kir6.2 in the absence of atrial or ventricular SUR1 (Fig. S1C and S1D) is indicative of SUR1-containing K_{ATP} channels in both chambers.

Curiously, ventricular SUR1 was consistently a faster migrating, Endo H-resistant electrophoretic species compared to atrial SUR1, indicative of differential complex glycosylation (Fig. 1D and E). PNGase F confirms that SUR1 is complex glycosylated in both chambers (Fig. 1F). Indeed, both atrial and ventricular SUR1 migrated faster and identically after PNGase F treatment confirming that differential atrial and ventricular SUR1 mobility is due to differential complex glycosylation.

Surprisingly, localization studies in isolated atrial and ventricular myocytes with antibodies against SUR1 and Kir6.2 (Fig. S2A-C demonstrates antibody specificity in the native cardiac environment using knockout controls for the respective antigen) reveal that SUR1-containing K_{ATP} channels are differentially localized when comparing atrial and ventricular myocytes: SUR1 and Kir6.2 co-localize at the plasma membrane of atrial myocytes (Fig. 2A, left panel). SUR2A was visible at the cell surface of ventricular myocytes (Fig. 1B), but SUR1 was not at the plasma membrane, nor in T tubules. Instead, SUR1 was mostly retained in intracellular structures where it co-localized with Kir6.2 (Fig. 2A, right panel). We confirmed this difference in SUR1 surface localization between atria and ventricles by a complementary biochemical method (Fig. 2B, C), i.e. labeling of cell-surface exposed

SUR1 using extracellular cysteine PEGylation (Fig. 2D, E demonstrates specific labeling of only the complex-glycosylated form of SUR1 upon co-expression with Kir6.2 in HEK293 cells). The sodium-calcium exchanger NCX1 is an established control protein for extracellular cysteine PEGylation in cardiac myocytes (Fig. 2B) (Shen et al., 2007), and is present at ventricular T-tubules and plasma membrane of both atrial and ventricular myocytes (Jayasinghe et al., 2009). NCX1 labeled with similar efficacy in both cell types implying that all regions of the cell surface were accessible to the PEGylation reagent. In contrast, SUR1 labeled at least threefold more extensively in atrial than in ventricular myocytes (Fig. 2B,C), supporting the conclusion that more SUR1 is present at the plasma membrane of atrial than ventricular myocytes.

In *knj11*^{-/-} hearts, SUR1 was retained intracellularly, in punctate structures throughout the cell but predominantly in a juxtannuclear compartment (inset, Fig. S2A). Conversely, the cell surface of atrial *abcc8*^{-/-} myocytes was devoid of specific Kir6.2 staining and the remaining Kir6.2 protein was all detected inside the cell (inset, Fig. S2B). In ventricular *abcc8*^{-/-} myocytes, weak cell surface and striated Kir6.2 staining, presumably T-tubular, was still visible (Fig. S2B), in line with SUR2A being the only partner subunit in the absence of SUR1 (Fig. 1A,B and S1B). We therefore conclude that SUR1 assembles with Kir6.2 in both atrial and ventricular myocytes. However, SUR1-containing K_{ATP} complexes are expressed at the cell surface of atrial myocytes but predominantly intracellular in ventricular myocytes.

Differential complex glycosylation of ventricular SUR reflects Golgi retention

Faster electrophoretic migration of ventricular SUR1 that disappeared upon PNGase F treatment (Fig. 1), and lack of SUR1 at the ventricular myocyte surface (Fig. 2), may result from differential complex glycosylation, which we addressed using different glycosidases. We also assessed the electrophoretic mobility of other glycoproteins in atria and ventricles (Fig. 3A): The cardiac sodium channel Na_v1.5 (Stocker and Bennett, 2006), the β₁-adrenergic receptor (β₁-AR, (Rohrer et al., 1996)) and β-dystroglycan (β-DG, (Holt et al., 2000)) were present in both atrial and ventricular membranes. Interestingly, atrial Na_v1.5 exhibited a migratory shift similar to that of SUR1 whereas β₁-AR and β-DG glycoproteins migrated identically in atria and ventricles. This suggests that tissue-specific differential glycosylation observed for

SUR1 and Na_v1.5 is restricted to only a subset of cargo proteins of the secretory pathway.

Co-localization analysis of SUR1 and the vesicle docking protein p115 (Nakamura et al., 1997), a marker of the cis-Golgi (Fig. 3B), identified the majority of ventricular SUR1-containing K_{ATP} channels in the Golgi, either juxtannuclear or scattered throughout both atrial and ventricular myocytes ((Fawcett and McNutt, 1969) and Fig. S2D). Treatment with neuraminidase, which cleaves glycosidic linkages of sialic acids, increased the electrophoretic mobility of atrial SUR1, which now migrated close to the untreated, ventricular form (Fig. 3C) indicating that atrial SUR1 is modified by sialic acid residues. Ventricular SUR1 was minimally affected by neuraminidase treatment, suggesting that both SUR1 forms carry the specific sugar moieties recognized by this exoglycosidase, but to different degrees. Since protein sialyl-transferases are present in medial and trans-Golgi compartments (Zhao et al., 2006) this implies that ventricular SUR1-containing K_{ATP} channels move at least as far as the medial Golgi, from where they are presumably retrieved due to recognition by the COPI-coat (Michelsen et al., 2007; Zerangue et al., 1999). Consistent with differential electrophoretic mobility shift upon neuraminidase treatment, both atrial and ventricular SUR1 and Na_v1.5 bound wheat germ agglutinin (WGA), which specifically binds to N-acetyl-glucosamine, neuraminic and sialic acid (Fig. 3D). Notably, the complement of proteins eluted from the WGA matrix was similar between atrial and ventricular proteins (Fig. 3E) suggesting that differential glycosylation is limited to only a subset of WGA-binding proteins. Thus, differences in SUR1 and Nav1.5 migratory behaviors may reflect different residence times in medial and trans-Golgi compartments, due to retrieval of these select cargo proteins. We conclude that Kir6.2/SUR1 complexes are retained within the Golgi, specifically in ventricular but not atrial myocytes. We also show that Na_v1.5 is an independent and functionally essential cargo protein that is differentially glycosylated. Thus, the secretory pathways of atrial and ventricular myocytes may differentially control the trafficking of additional membrane proteins.

Channel deployment in response to β -adrenergic stimulation

In heterologous expression, SUR1-containing K_{ATP} channels are more sensitive to activation by Mg-nucleotide diphosphates (Mg-ADP) than are SUR2A-containing

channels (Masia et al., 2005). Hence Golgi-retained SUR1-containing channels may provide a fully assembled pool of channels that if subsequently trafficked to the cell surface could provide enhanced metabolism sensing and protection from deleterious consequences of energy depletion. Kir6.2-containing K_{ATP} channels are known to contribute to action potential shortening during catecholaminergic stress mediated by β -adrenergic receptors (Zingman et al., 2002), but the SUR composition of these channels is unknown. We applied the selective β -adrenergic agonist isoproterenol (ISO) together with the cAMP-specific phosphodiesterase type 4 inhibitor rolipram (ROL) for 1 hour in intact hearts. In ventricular myocytes isolated from treated hearts, we observed significant spatial reorganization of the dispersed (Fig. 2A and 4A ‘control’) SUR1 signal into regular striation-associated fluorescence (Fig. 4A, B and C). This raises the possibility that SUR1-containing K_{ATP} channels are inserted into the cell surface membrane, particularly into T-tubule membranes. Notably, the spatial distribution of the sodium-calcium exchanger NCX1, which localizes to the plasma membrane of ventricular myocytes within and outside T-tubules, was not affected by sustained beta-adrenergic stimulation (Fig. S3A-C), but overlapped with SUR1 after treatment with ISO/ROL (Fig. S3D). These findings are consistent with cAMP-dependent translocation of SUR1-containing K_{ATP} channels to T tubules.

The potassium channel opener diazoxide potently activates SUR1-containing K_{ATP} channels but not SUR2A-containing channels, whereas pinacidil activates SUR2A-, but not SUR1-containing channels (Flagg et al., 2008). Consistent with the above hypothesis, ISO/ROL treatment significantly increased the diazoxide-sensitive component, but not the pinacidil-sensitive component, of the K_{ATP} channel current in wt ventricular myocytes treated with the same protocol (Fig. 4D). The mean total K_{ATP} current was not significantly increased (Fig. 4E) although individual myocytes exhibited larger total K_{ATP} currents. Levels of SUR1, Kir6.2 and 14-3-3 as well as the phosphorylation status of phospholamban, a well-characterized target of protein kinase A (PKA, a major effector of β -adrenergic signal transduction) (Fig. 4F; see Fig. S3E for quantification) confirmed increased activation of β -adrenergic effectors and excluded increased total SUR1 or Kir6.2 as an explanation for the presence of SUR1-containing K_{ATP} channels at the ventricular myocyte surface.

Abundance of 14-3-3 correlates with channel trafficking

K_{ATP} channels belong to a group of cargo proteins that recruit 14-3-3 proteins, yet where in the cell this occurs is unknown (Heusser et al., 2006). 14-3-3-dependent cargo proteins TASK-1 (another potassium channel) and ADAM22 (a catalytically inactive metalloprotease) both accumulate in cis- and medial- but not trans-Golgi compartments in the absence of 14-3-3 interaction (Godde et al., 2006; Zuzarte et al., 2009) and we hypothesize that ventricular SUR1/Kir6.2 K_{ATP} channels lack sufficient 14-3-3 protein interactions during intra-Golgi trafficking, resulting in constitutive Golgi localization (Fig. 2) and reduced sialylation (Fig. 3). 14-3-3 protein levels were markedly lower in ventricular than atrial myocytes (Fig. 5A and B), raising the possibility that reduced 14-3-3 protein availability limits cell surface expression of SUR1/Kir6.2 K_{ATP} channels in ventricles. Immunofluorescence staining of atrial myocytes using a pan-14-3-3 isoform antibody revealed strong labeling of juxtannuclear, submembraneous and intracellular compartments, including a weak striated pattern (Fig. 5C, AM). In ventricular myocytes, 14-3-3 immunostaining was much weaker (compare Fig. S2D) and primarily restricted to intracellular striations (Fig. 5C, VM), suggestive of a specific association with Z-lines and T-tubule junctions of the ER. In both atrial and ventricular myocytes, there was significant co-localization of 14-3-3 with p115 (Fig. 5C), adjacent to Z lines of ventricular myocytes (Fig. 5D), suggesting that cardiac 14-3-3 proteins are present at the Golgi apparatus and consistent with overlapping immunofluorescence patterns for GM130, a p115-interacting Golgi matrix protein (Nakamura et al., 1997), and 14-3-3 in HeLa cells (Preisinger et al., 2004). Intriguingly, the localization of these Golgi elements in the vicinity of Z lines coincides with the observation that coated vesicles are frequently observed in this region, but only sometimes connected to the ER (Fawcett and McNutt, 1969). Co-localization of K_{ATP} channels with p115 and differential sialylation of atrial and ventricular SUR1 (Fig. 3) imply that the channel complexes are stalled in Golgi elements, possibly as part of a dedicated secretory pathway between ER and T-tubules at Z lines.

Six mammalian 14-3-3 isoforms were expressed in isolated myocytes, most abundantly 14-3-3 epsilon and eta, but ventricular myocytes expressed less of every isoform (35 to 75% mRNA) compared to atrial myocytes (Fig. 5E), consistent with specific retention of ventricular K_{ATP} channels being due to significantly reduced

abundance of all 14-3-3 isoforms. The present results raise the novel possibility that in terminally differentiated cell types, such as cardiac myocytes, the availability of 14-3-3 proteins may be important in regulation of surface expression of specific cargoes, and that 14-3-3 availability may underlie differences in the expression of functionally important cell-surface proteins.

Silencing of Arg-based signals by phosphorylation

We hypothesize further that a direct action of PKA induces cell surface trafficking of the SUR1/Kir6.2 complexes, in addition to its direct activating effects on channel function in heterologous overexpression systems (Beguin et al., 1999). Immunoprecipitation using an antibody that recognizes phosphorylated PKA-target motifs, strongly enriched Kir6.2 from solubilized membranes that were prepared from animals treated with ISO/ROL as compared to control animals (Fig. 6 A,B). Affinity purification of all phosphorylated proteins present in solubilized membranes by phos-tag affinity chromatography (Fig. S4 A-C), confirmed phosphorylation of Kir6.2. Importantly, the anti-PKA phospho-substrate antibody blocked binding of Kir6.2 from treated animals to the phos-tag matrix. Thus we conclude that sustained β -adrenergic stimulation results in PKA-dependent phosphorylation of cardiac Kir6.2. Next, we tested the possible consequences of Kir6.2 phosphorylation by PKA on channel trafficking by an in vitro binding experiment to capture the inherently transient interaction with trafficking machinery such as the COPI vesicle coat. Upon exposure of the C-terminal 36 amino acids of Kir6.2 to the catalytic subunit of PKA, the peptide was phosphorylated (Fig. S4D). The same activity was confirmed for endogenous PKA present in cardiac cytosol and total membranes (Fig. S4E) demonstrating that cardiac PKA forms can target the C-terminus of Kir6.2. Interestingly, phosphorylation of the Kir6.2 C-terminal peptide strongly reduced the binding of both COPI and 14-3-3 (Fig. 6C and 6D and S5). Recombinant channel assays have shown that this consensus PKA phosphorylation site (S372, Fig. S4A) can be phosphorylated (Beguin et al., 1999). Beguin et al. reported that this underlies PKA-enhancement of gating, whereas Lin et al. (2000) reported that PKA-dependent gating was unaffected by mutation at this site. Thus we cannot exclude an effect of such phosphorylation on gating, but the present data clearly suggest a significant effect on trafficking.

Although many 14-3-3-binding sites depend on phosphorylation of a serine that is part of the consensus binding-motif, negative effects of the phosphorylation of flanking serines on 14-3-3 binding have been described in a few other proteins (Waterman et al., 1998). This suggests that PKA-phosphorylated channels may be released from COPI-dependent retrieval, losing the requirement for 14-3-3 binding, and hence exiting the Golgi irrespective of 14-3-3 availability (Fig. 6E).

SUR1-containing K_{ATP} channels contribute to action potential duration during sustained β -adrenergic stimulation

K_{ATP} channel activation and decreased action potential duration (APD) can occur during sustained β -adrenergic stimulation (Zingman et al., 2002), but SUR composition of these channels is unknown. In the light of our observation that a ventricular population of SUR1-containing K_{ATP} channels can translocate to the T tubule surface upon β -adrenergic signaling we tested whether SUR1-containing channels might play a role in APD shortening. To this end we performed optical mapping of action potentials in wt and *abcc8*^{-/-} hearts (Fig. 7A-C) under control conditions, after treatment with ISO/ROL and after the same treatment in the presence of glibenclamide, which blunts the K_{ATP} channel contribution to action potential shortening (Zingman et al., 2002). Intriguingly, APD in *abcc8*^{-/-} mice was unaffected by treatment with ISO/ROL alone or in combination with glibenclamide, in contrast to wt hearts where we confirmed the observations by Zingman et al. (Zingman et al., 2002). This result delineates a physiological role for the PKA-regulated cell surface translocation of SUR1-containing channels during sustained β -adrenergic stimulation (Figs. 4,6).

DISCUSSION

Our experiments provide novel insights into the cellular control of localization and trafficking of an important ion channel complex in terminally differentiated cardiac myocytes (Fig. 8). SUR1-containing K_{ATP} channels constitutively reach the cell surface only in atrial myocytes (Fig. 2), potentially because of the high abundance of 14-3-3 proteins (Fig. 5), which are required to overcome the COPI-dependent retrieval signals present in Kir6.2 and SUR1 (Heusser et al., 2006; Michelsen et al., 2005; Yuan et al., 2003). In contrast, SUR1-containing K_{ATP} channels are stalled in the Golgi of ventricular myocytes but are deployed to the cell surface upon sustained β -adrenergic stimulation (Fig. 2,3,4). Interestingly, SUR2A-containing channels constitutively reach the plasma membrane in ventricular myocytes, despite the low abundance of 14-3-3 proteins (Fig. 1,5). Based on the consensus of Arg-based signals, SUR2 contains a less potent ER retrieval signal (RKQ) than SUR1 (RKR) (Konstas et al., 2002; Michelsen et al., 2005; Zerangue et al., 2001) possibly making SUR2A-containing K_{ATP} channels less dependent on 14-3-3. Upon phosphorylation of the C-terminus of Kir6.2, both COPI and 14-3-3 cease to interact with the protein (Fig. 6, S4, S5), potentially releasing the channel from COPI- and 14-3-3-dependent control of anterograde trafficking. Importantly, newly integrated SUR1-containing K_{ATP} channels in the T-tubule surface will be intrinsically more sensitive to metabolic activation than SUR2A containing channels (Masia et al., 2005) and are likely to be highly active due to phosphorylation by PKA (Beguin et al., 1999). We identify a physiological role for this SUR1-containing channel population in action potential shortening during sustained β -adrenergic stimulation (Fig. 7). Our results are consistent with previous reports demonstrating K_{ATP} channel contribution to action potential shortening under these conditions (Zingman et al., 2002), but clarify the K_{ATP} channel subunits involved and indicate that the phenomenon may rely on PKA-regulated deployment of SUR1-containing channels to the ventricular cell surface in T tubules.

Our results identify a novel molecular mechanism that utilizes COPI-dependent storage in the Golgi for the regulated cell surface expression of a key cargo protein. Strikingly, most characterized Arg-based retrieval signals are flanked by serines, some of which are known targets of phosphorylation (Table S2). Thus, interaction with COPI coat proteins may - in addition to providing an assembly checkpoint - be

harnessed in terminally differentiated cell types to allow regulated deployment from the Golgi to the cell surface. COPI-dependent storage and regulated deployment may then explain conflicting results that imply activity of Arg-based signals in retrieval as well as exit from the early secretory pathway (compare references in Table S2). We suggest a mechanism how SUR1-containing K_{ATP} channels may be released from COPI- and 14-3-3-dependent control, and hence play a previously unrecognized role in the cAMP-dependent ‘fight-or-flight’ response of the heart (Fig. 7 and 8). SUR1-containing channels are very sensitive to block by sulfonylureas, lending additional weight to clinical recommendations that call for the re-evaluation of the cardiac risk associated with sulfonylurea treatment in type II diabetes (Gore and McGuire, 2011; Schramm et al., 2011).

MATERIALS AND METHODS

Mice

Wild-type (wt), Kir6.2 knockout (*kcnj11*^{-/-}; Miki et al. 1998) and sulfonylurea receptor type-1 (SUR1) knockout (*abcc8*^{-/-}; Shiota et al. 2002) mice, all male in the C57BL/6J background, aged 8-14 weeks, were used.

Cardiac tissue and myocyte preparation

Hearts were retrogradely perfused by a modified Langendorff solution (NaCl 120.4 mM, KCl 14.7 mM, KH₂PO₄ 0.6 mM, Na₂HPO₄ 0.6 mM, MgSO₄ 1.2 mM, Na-HEPES 10 mM, NaHCO₃ 4.6 mM, taurine 30 mM, 2,3-butanedione-monoxime 10 mM, glucose 5.5 mM, pH 7.4) for a period of 4 min at 37°C at a flow rate of 4 ml/min. For isolation of cardiomyocytes, perfusion included collagenase type II (600 U/ml). Residual tissue was removed by a 100 µm cell strainer (BD Falcon, 352360). 10% bovine calf serum and 12.5 µM CaCl₂ in perfusion buffer inhibited collagenase activity. Isolated myocytes were plated on laminin-coated glass cover slips at 1500 cells/cm².

Indirect immunofluorescence microscopy

Mouse atrial or ventricular myocytes were fixed with 4 % PFA, washed 3x in PBS, and incubated overnight in blocking buffer (10 % bovine calf serum, 0.2 % Triton in PBS). Primary antibodies were diluted (see Table S1) in blocking buffer. Samples were incubated overnight at 4 °C, washed 3x in blocking buffer and incubated with Alexa-Fluor secondary antibodies (Invitrogen) for 2 h at room temperature.

Image acquisition and co-localization analysis

All images were acquired with a confocal microscope (Zeiss LSM 710, Jena, Germany) using the Plan-Apochromat 63x/1.40 Oil DIC M27 objective. All images were analyzed by ImageJ software (imagej.nih.gov). Co-localization analysis was performed by applying intensity correlation analysis (Li et al., 2004) on ROIs generating colocalization maps and the intensity correlation quotient (ICQ), with positive values (0-0.5) indicating co-dependent staining.

Fourier transform analysis

20 untreated and 18 isoproterenol/rolipram treated ventricular myocytes from four hearts were immunostained for SUR1. Confocal sections were selected omitting cell nuclei. T-tubule associated transverse striation pattern was aligned with the image y-axis by virtual image rotation. Fast Fourier transformation was performed from equally sized ROIs (~ 36 Z-lines) using ImageJ version 1.43u. The power of periodic frequencies along the image x-axis (longitudinal cell axis) was derived from the Fourier domain images (not shown). Binary images in Fig. 4A were obtained by thresholding the raw data images and visualizing the alteration in spatial signal organization upon β -adrenergic stimulation.

Immuno-transmission electron microscopy

Mouse hearts were dissected and perfused for 4 min with perfusion buffer followed by 5 min perfusion with 4% paraformaldehyde in PBS pH 7.4 for fixation of cardiac tissue. Left ventricles were fixed for an additional 2 h in 4 % paraformaldehyde/PBS at RT followed by fixation in 2 % paraformaldehyde/PBS overnight at 4 °C. Fixed ventricles were cut into small blocks, infused with 2.3 M sucrose/PBS at 4 °C overnight, mounted on metal pins in an orientation allowing sectioning in the longitudinal axes. Ultrathin (75 nm) longitudinal cryosections were prepared according to the Tokuyasu method (Tokuyasu, 1973). For immuno-labeling, sections were blocked with 1 % BSA/TBS and incubated with anti-p115 antibody followed by 10 nm gold-coupled anti-mouse secondary antibody (Aurion). Following 5 min cross-linking using 1 % glutaraldehyde/PBS, sections were probed with anti-14-3-3 antibody and then 6 nm gold-coupled anti-mouse secondary antibody (Aurion). Sections were contrasted with 0.4 % (w/v) uranyl acetate in 2 M methyl-cellulose for 15 min on ice, embedded in the same solution and examined with a Phillips CM120 transmission electron microscope. Micrographs were acquired with a CCD camera (Megaview III, Olympus Soft Imaging Systems) and processed using iTEM software.

mRNA analysis

Three rat hearts were used to extract RNA from atrial and ventricular myocytes. Total RNA was extracted by the Trizol method (Invitrogen), treated with DNase I (TURBO DNase, 2 U/ μ l, Invitrogen) and further purified by phenol/chloroform/isoamyl alcohol extraction and subsequent ethanol precipitation. cDNA was obtained by reverse

transcription (qScript cDNA SuperMix, Quanta BioSciences). Quantitative real-time PCR was performed using an iQ5 cycler (Bio Rad) and PerfeCTa SYBR Green SuperMix (Quanta BioSciences). Primer sequences are available upon request. The mRNA values were normalized to the corresponding GAPDH mRNA.

Statistics

Data are presented as mean±standard error of the mean (S.E.M.). Differences between experimental groups were tested for statistical significance using unpaired two-tailed Student's t-test. P-values <0.05 were considered significant.

Western blot detection

Primary antibodies were diluted (as described in Table S1) in blocking buffer (5 % w/v milk powder, 25 mM Tris/HCl pH 7.4, 135 mM NaCl, 3 mM KCl, 0.02 % NP-40). The blots were imaged using an Odyssey® Sa Infrared imaging system (IRDye LiCOR- secondary antibody).

Crude Membrane Preparation

Tissue was equilibrated in ice-cold homogenization buffer (50 mM NaCl, 0.32 M sucrose, 2 mM EDTA, 20 mM HEPES pH 7.4) containing protease inhibitors and homogenized using a Micra D-1 homogenizer. Cleared supernatant was centrifuged at ~100,000 g to yield cytosol and a membrane pellet.

Membrane solubilization

Membranes were solubilized at 1 mg total protein/ml solubilization buffer (1.5 % Triton X-100, 0.75 % Na-Deoxycholate, 0.1 % SDS in 10 mM NaCl, 5 mM EDTA, 2.5 mM EGTA and 50 mM Tris/HCl pH 7.35) containing protease inhibitors. The solubilized extracts were centrifuged at 50,000 g, supernatants TCA-precipitated, acetone washed, and the pellet resuspended in 1x SDS sample buffer. Unless stated otherwise, the SDS sample buffer contained 100 mM DTT.

Glycosidase treatment

Membranes (~100 µg total protein) were solubilized and re-suspended in reaction buffer (G1, G5 or G7 as appropriate and supplied as 10X buffers by New England

BioLabs Inc.) and 0.25 % NP-40 in a final volume of 40 μ l. 2.5 μ l (125 U) of Neuraminidase, 1 μ l (500 U) of EndoH and 1 μ l (500 U) of PNGaseF were used per reaction (37 °C for 1 hour).

Lectin binding assay

The resin (Agarose-conjugated *Triticum vulgare* lectin) was incubated with wash buffer (150 mM NaCl, 2mM EDTA, 2mM EGTA, 20 mM HEPES pH 6.8) for 5 min, washed 5x in equilibration buffer (150 mM NaCl, 5 mM MnCl₂, 5 mM MgCl₂, 5 mM CaCl₂, 20 mM Tris pH 7.4) and once in solubilization buffer. Membranes prepared from rat tissues were solubilized at 1 mg total protein/ml in solubilization buffer (10 mM NaCl, 1.5% TX-100, 50 mM Tris-HCl pH7.35). 400 μ l of solubilized membrane extract (400 μ g protein) was incubated with ~50 μ l gravity-settled resin for 5 hours at 4 °C. The resin was washed 6x in wash buffer (150 mM NaCl, 2.5 mM MnCl₂, 2.5 mM MgCl₂, 2.5 mM CaCl₂, 50 mM Tris pH 7.4). Bound proteins were eluted with 1x SDS Sample buffer.

Mal-PEG cell surface labeling assay

The method established by Shen et al (2007) was adapted as follows: Transfected HEK293T cells were washed twice with PBS. Cell surface-exposed cysteines were reduced using 6 mM TCEP (tris(2-carboxyethyl) phosphine) in serum free DMEM (pH adjusted to 7.0) and incubated at 4 °C for 15 minutes. Cells were washed twice with serum-free DMEM. Maleimide-conjugated polyethylene glycol (Mal-PEG; Mol. Wt. 5000 Da, Iris biotech GmbH) was purified by gel filtration on a PD-10 column. 500 μ l of 5 mM Mal-PEG solution was used per well of a 6 well multiwell cell culture plate. After 30 minutes at 4 °C, two washes in serum-free DMEM, quenching with 5 mM NEM (N-Ethylmaleimide), cells were re-suspended in solubilization buffer (500 mM 6-aminohexanoic acid, 1 mM EDTA, 50 mM imidazole/HCl pH 7.0) containing 2.5 % w/v Digitonin and 5 mM NEM. The lysate was supplemented with 5x SDS-PAGE sample buffer (without DTT). For mouse hearts, the perfusion buffer was saturated with 100 % oxygen. Following an equilibration period of 2 minutes at 37 °C, cell surface-exposed cysteines were reduced using 6 mM TCEP in perfusion buffer (pH adjusted to 7.4) for 6 min at 23 °C followed by a 2 minute wash. The heart was subsequently perfused with 5 mM Mal-PEG in perfusion buffer for 6 minutes and

quenched by NEM (5 mM) for 5 minutes.

Recombinant Expression of Proteins and Purification from *E. coli*

Bait proteins used for binding assays were purified as described in Yuan et al. (2003).

Binding Assays

Purified bait proteins were phosphorylated with 5 ng recombinant PKA per reaction in reaction buffer (150 mM KOAc, 5 mM Mg(CH₃COO)₂, 2% Glycerol, 1 mM EDTA, 20 mM HEPES pH 7.4 and protease inhibitor) with ATP regeneration system (10 mM phosphocreatine, 0.5 mM ATP, 0.5 mM GTP, 50 µg/ml creatine phosphokinase) for 6 hours. 5 µM protein kinase-A inhibitor (PKI (5-24); Santa Cruz Biotechnology, Inc.) was used prior to PKA addition. Cytosol or total membranes containing 65 µg protein per reaction were added as indicated. Bait proteins (2.5 µg per reaction) were immobilized on IgG sepharose following phosphorylation and washed 5x with reaction buffer. An equimolar concentration of bait:MBP-14-3-3 ζ or bait:recombinant COPI was added, incubated for 6 hours, washed 5x with reaction buffer and eluted with R18 peptide (PHCVPRDLSWLDLEANMCLP, concentration 100 µM) for 14-3-3 binding or with 1x SDS sample buffer (without DTT) for the COPI binding assay. COPI coat was prepared (Sahlmuller et al., 2011). PKA was purified as described in Mant et al. (2011).

Phos-tag PAGE

Phos-tag Acrylamide (NARD institute, Ltd.) was used as per manufacturers' instructions (stock: 5 mM).

In vitro phosphorylation of membranes

Crude membranes were washed twice in stripping buffer (500 mM KCl, 5 mM EDTA, 5 mM EGTA, 50 mM Tris pH 7.4 including Protease inhibitors), then resuspended in phosphorylation buffer (150 mM NaOAc, 5 mM Mg(CH₃COO)₂, 20 mM Tris-OAc, pH 7.4) and phosphorylated using recombinantly purified PKA (5-10 ng/ reaction) in the presence of an ATP regeneration system or treated with calf intestinal alkaline phosphatase (2 U) in the presence of PKI (5 µM).

Immobilized metal affinity chromatography

Crude membranes were solubilized (30 minutes at 4°C) in Complexiolyte buffer 71 (Logopharm) (at 1 mg/ml) and centrifuged at 50,000 g. The extracts (containing ~75 μg total protein) were diluted 1:5 in phos-tag-agarose binding/wash buffer and incubated with (7 μg) of the indicated antibodies (#2729, #9624, Cell Signaling Technology) for a period of 30 minutes at 4°C, prior to use with the Phos-tag matrix. Phos-tag agarose (NARD institute, Ltd.) was used as per manufacturer's instructions.

Immunoprecipitation

10 μg affinity-purified rabbit antibodies (#2729, #9624, Cell Signaling Technology) were immobilised on Dynabeads (protein G) according to the manufacturers instructions (Life technologies). Crude mouse heart membranes were solubilized in Complexiolyte buffer 71 (1 mg/ml, 30 minutes at 4°C and centrifuged, 50,000 g for 15 minutes). The extracts (containing ~100 μg total protein per reaction) were diluted 1:5 in IP binding/wash buffer (150 mM KCl, 5 mM MgCl_2 , 20 mM Tris-HCl, pH 7.4, including protease inhibitors (Roche; Complete, EDTA free) and PhosSTOP phosphatase inhibitor (Roche) cocktail) and incubated with the affinity matrix for 30 minutes at 4°C. Following 4 washes, bound proteins were eluted with SDS sample buffer (without DTT).

Electrophysiology

Inside-out excised membrane patches were voltage-clamped at -50 mV (pipette voltage, $+50$ mV). Bath (intracellular) and pipette (extracellular) solution had the following composition: 140 mM KCl, 10 mM HEPES, 1 mM EGTA, pH 7.3 (K_{int} solution). Working concentrations- 100 μM ATP plus 5 mM Mg^{2+} ; 300 μM diazoxide or pinacidil. Data are presented as stimulated I_{rel} (relative current amplitude in diazoxide or pinacidil, normalized to maximum K_{ATP} current in zero ATP). Data were acquired using pClamp 8.2 software suite (Axon Instruments), and analyzed using ClampFit and Microsoft Excel software. Data from myocytes pretreated with 10 μM isoproterenol and 10 μM rolipram for 1-2 hours (labeled as 'ISO') were recorded in K_{int} solution under the same conditions as described above.

Optical measurements of action potential duration

Isolated heart preparations were performed as described (Glukhov et al., 2009). After isolation, cannulation, motion suppression, and dye staining, preparations were equilibrated for an additional 5-10 min before imaging of control measurements during spontaneous rhythm and ventricular pacing. Hearts were paced at the lateral right ventricular (RV) epicardium; pacing current was 2× diastolic pacing threshold. After control measurements, ISO/ROL (final concentration 10 μ M each) were introduced to both superfusion and perfusion lines. Sinus-driven and ventricular-paced recordings were obtained at 5 minute intervals for 20 minutes, following which glibenclamide (10 μ M) was added to the Tyrode's solution containing ISO/ROL. A customized Matlab-based computer program (Laughner et al., 2012) was used to analyze optical signals, which were filtered using a 3x3 pixel spatial filter and a 0-175 Hz finite impulse response filter. Activation times at the maximum first derivative (dV/dt_{\max}) of optical action potentials were calculated using normalized optical signals. APD was measured as the interval from activation time to 80% repolarization (APD80%), during continuous pacing for each pixel and then averaged throughout the ventricle. Values are expressed as means \pm SE unless otherwise stated. Statistical analysis was performed using one-way ANOVA followed by Tukey's post hoc comparison of means. A value of $p < 0.05$ was considered statistically significant.

ACKNOWLEDGMENTS

We thank F. Matthes, B. Schumann, B. Korff, P. Mannheim, and K. Unthan-Fechner for excellent technical support; B. Brügger, I. Reckmann, F. Wieland for COPI subunit-specific antibodies and COPI coat; M. Kilisch, O. Lytovchenko for purified PKA and 14-3-3; I. O'Kelly, P. Evers for a PKA expression construct; S. Seino, M. A. Magnuson for access to mouse lines; A. Kaul, B. Liss for help with establishing the Kir6.2 ko line in Göttingen; T. Harter for maintenance of animal lines in Saint Louis. D. Riedel, D. Wenzel, G. Heim for technical advice on electron microscopy. We thank D. Attwell, J. Daut, D. Doenecke, R. Kehlenbach, G. Hasenfuß, S. High, T. Jentsch, A. J. Smith for extremely helpful comments. We are grateful for financial support from a Wellcome Trust Senior Research Fellowship to BIS and from DFG SFB 1002 TP B01 to BIS and DFG SFB 1002 TP A05 to SEL, KFO 155, BMBF NGFN+, FP7 EUTrigTreat to SEL, from NIH grant HL95010 to CGN. SB was financially supported by Jacob-Henle-Programm, University Medicine Göttingen, and Studienstiftung des dt. Volkes.

REFERENCES

- Abe, K., and R. Puertollano. 2011. Role of TRP channels in the regulation of the endosomal pathway. *Physiology (Bethesda)*. 26:14-22.
- Babenko, A.P., G. Gonzalez, L. Aguilar-Bryan, and J. Bryan. 1998. Reconstituted human cardiac KATP channels: functional identity with the native channels from the sarcolemma of human ventricular cells. *Circ Res*. 83:1132-1143.
- Beguín, P., K. Nagashima, M. Nishimura, T. Gonoï, and S. Seino. 1999. PKA-mediated phosphorylation of the human K(ATP) channel: separate roles of Kir6.2 and SUR1 subunit phosphorylation. *EMBO J*. 18:4722-4732.
- Bezzlerides, V.J., I.S. Ramsey, S. Kotecha, A. Greka, and D.E. Clapham. 2004. Rapid vesicular translocation and insertion of TRP channels. *Nature cell biology*. 6:709-720.
- Bogan, J.S. 2012. Regulation of glucose transporter translocation in health and diabetes. *Annual review of biochemistry*. 81:507-532.
- Conti, L.R., C.M. Radeke, and C.A. Vandenberg. 2002. Membrane targeting of ATP-sensitive potassium channel. Effects of glycosylation on surface expression. *J Biol Chem*. 277:25416-25422.
- Fawcett, D.W., and N.S. McNutt. 1969. The ultrastructure of the cat myocardium. I. Ventricular papillary muscle. *J Cell Biol*. 42:1-45.
- Flagg, T.P., H.T. Kurata, R. Masia, G. Caputa, M.A. Magnuson, D.J. Lefer, W.A. Coetzee, and C.G. Nichols. 2008. Differential structure of atrial and ventricular KATP: atrial KATP channels require SUR1. *Circ Res*. 103:1458-1465.
- Garratt, K.N., P.A. Brady, N.L. Hassinger, D.E. Grill, A. Terzic, and D.R. Holmes, Jr. 1999. Sulfonylurea drugs increase early mortality in patients with diabetes mellitus after direct angioplasty for acute myocardial infarction. *J Am Coll Cardiol*. 33:119-124.
- Glukhov, A.V., T.P. Flagg, V.V. Fedorov, I.R. Efimov, and C.G. Nichols. 2009. Differential K(ATP) channel pharmacology in intact mouse heart. *J Mol Cell Cardiol*. 48:152-160.
- Godde, N.J., G.M. D'Abaco, L. Paradiso, and U. Novak. 2006. Efficient ADAM22 surface expression is mediated by phosphorylation-dependent interaction with 14-3-3 protein family members. *J Cell Sci*. 119:3296-3305.
- Goldner, M.G., G.L. Knatterud, and T.E. Prout. 1971. Effects of hypoglycemic agents on vascular complications in patients with adult-onset diabetes. 3. Clinical implications of UGDP results. *JAMA*. 218:1400-1410.
- Gore, M.O., and D.K. McGuire. 2011. Resolving drug effects from class effects among drugs for type 2 diabetes mellitus: more support for cardiovascular outcome assessments. *European heart journal*. 32:1832-1834.
- Henry, R.R. 1998. Type 2 diabetes care: the role of insulin-sensitizing agents and practical implications for cardiovascular disease prevention. *Am J Med*. 105:20S-26S.
- Heusser, K., H. Yuan, I. Neagoe, A.I. Tarasov, F.M. Ashcroft, and B. Schwappach. 2006. Scavenging of 14-3-3 proteins reveals their involvement in the cell-surface transport of ATP-sensitive K⁺ channels. *J Cell Sci*. 119:4353-4363.
- Holt, K.H., R.H. Crosbie, D.P. Venzke, and K.P. Campbell. 2000. Biosynthesis of dystroglycan: processing of a precursor propeptide. *FEBS Lett*. 468:79-83.
- Isidoro Tavares, N., P. Philip-Couderc, A.J. Baertschi, R. Lerch, and C. Montessuit. 2009. Angiotensin II and tumour necrosis factor alpha as mediators of ATP-

- dependent potassium channel remodelling in post-infarction heart failure. *Cardiovasc Res.* 83:726-736.
- Isidoro Tavares, N., P. Philip-Couderc, I. Papageorgiou, A.J. Baertschi, R. Lerch, and C. Montessuit. 2007. Expression and function of ATP-dependent potassium channels in late post-infarction remodeling. *J Mol Cell Cardiol.* 42:1016-1025.
- Jayasinghe, I.D., M.B. Cannell, and C. Soeller. 2009. Organization of ryanodine receptors, transverse tubules, and sodium-calcium exchanger in rat myocytes. *Biophysical journal.* 97:2664-2673.
- Konstas, A.A., J.P. Koch, S.J. Tucker, and C. Korbmacher. 2002. Cystic fibrosis transmembrane conductance regulator-dependent up-regulation of Kir1.1 (ROMK) renal K⁺ channels by the epithelial sodium channel. *J Biol Chem.* 277:25377-25384.
- Korchev, Y.E., Y.A. Negulyaev, C.R. Edwards, I. Vodyanoy, and M.J. Lab. 2000. Functional localization of single active ion channels on the surface of a living cell. *Nature cell biology.* 2:616-619.
- Kornfeld, R., and S. Kornfeld. 1985. Assembly of asparagine-linked oligosaccharides. *Annual review of biochemistry.* 54:631-664.
- Laughner, J.I., F.S. Ng, M.S. Sulkin, R.M. Arthur, and I.R. Efimov. 2012. Processing and analysis of cardiac optical mapping data obtained with potentiometric dyes. *Am J Physiol Heart Circ Physiol.* 303:H753-765.
- Lehnart, S.E., X.H. Wehrens, S. Reiken, S. Warriar, A.E. Belevych, R.D. Harvey, W. Richter, S.L. Jin, M. Conti, and A.R. Marks. 2005. Phosphodiesterase 4D deficiency in the ryanodine-receptor complex promotes heart failure and arrhythmias. *Cell.* 123:25-35.
- Li, Q., A. Lau, T.J. Morris, L. Guo, C.B. Fordyce, and E.F. Stanley. 2004. A syntaxin 1, Galpha(o), and N-type calcium channel complex at a presynaptic nerve terminal: analysis by quantitative immunocolocalization. *J Neurosci.* 24:4070-4081.
- Lin, Y.F., Y.N. Jan, and L.Y. Jan. 2000. Regulation of ATP-sensitive potassium channel function by protein kinase A-mediated phosphorylation in transfected HEK293 cells. *EMBO J.* 19:942-955.
- Mant, A., D. Elliott, P.A. Eyers, and I.M. O'Kelly. 2011. Protein kinase A is central for forward transport of two-pore domain potassium channels K2P3.1 and K2P9.1. *J Biol Chem.* 286:14110-14119.
- Masia, R., D. Enkvetchakul, and C.G. Nichols. 2005. Differential nucleotide regulation of KATP channels by SUR1 and SUR2A. *J Mol Cell Cardiol.* 39:491-501.
- Michelsen, K., V. Schmid, J. Metz, K. Heusser, U. Liebel, T. Schwede, A. Spang, and B. Schwappach. 2007. Novel cargo-binding site in the beta and delta subunits of coatomer. *J Cell Biol.* 179:209-217.
- Michelsen, K., H. Yuan, and B. Schwappach. 2005. Hide and run. Arginine-based endoplasmic-reticulum-sorting motifs in the assembly of heteromultimeric membrane proteins. *EMBO reports.* 6:717-722.
- Miki, T., K. Nagashima, F. Tashiro, K. Kotake, H. Yoshitomi, A. Tamamoto, T. Gono, T. Iwanaga, J. Miyazaki, and S. Seino. 1998. Defective insulin secretion and enhanced insulin action in KATP channel-deficient mice. *Proc Natl Acad Sci U S A.* 95:10402-10406.

- Miki, T., M. Suzuki, T. Shibasaki, H. Uemura, T. Sato, K. Yamaguchi, H. Koseki, T. Iwanaga, H. Nakaya, and S. Seino. 2002. Mouse model of Prinzmetal angina by disruption of the inward rectifier Kir6.1. *Nat Med.* 8:466-472.
- Morrison, D.K. 2009. The 14-3-3 proteins: integrators of diverse signaling cues that impact cell fate and cancer development. *Trends Cell Biol.* 19:16-23.
- Nakamura, N., M. Lowe, T.P. Levine, C. Rabouille, and G. Warren. 1997. The vesicle docking protein p115 binds GM130, a cis-Golgi matrix protein, in a mitotically regulated manner. *Cell.* 89:445-455.
- Nichols, C.G., G.K. Singh and D.K. Grange. 2013, KATP Channels and Cardiovascular Disease. Suddenly a Syndrome. *Circ Res.* 112:1059-1072.
- Nichols, C.G. 2006. KATP channels as molecular sensors of cellular metabolism. *Nature.* 440:470-476.
- O'Kelly, I., M.H. Butler, N. Zilberberg, and S.A. Goldstein. 2002. Forward transport. 14-3-3 binding overcomes retention in endoplasmic reticulum by dibasic signals. *Cell.* 111:577-588.
- O'Kelly, I., and S.A. Goldstein. 2008. Forward Transport of K2p3.1: mediation by 14-3-3 and COPI, modulation by p11. *Traffic.* 9:72-78.
- Okuyama, Y., M. Yamada, C. Kondo, E. Satoh, S. Isomoto, T. Shindo, Y. Horio, M. Kitakaze, M. Hori, and Y. Kurachi. 1998. The effects of nucleotides and potassium channel openers on the SUR2A/Kir6.2 complex K⁺ channel expressed in a mammalian cell line, HEK293T cells. *Pflugers Arch.* 435:595-603.
- Philip-Couderc, P., N.I. Tavares, A. Roatti, R. Lerch, C. Montessuit, and A.J. Baertschi. 2008. Forkhead transcription factors coordinate expression of myocardial KATP channel subunits and energy metabolism. *Circ Res.* 102:e20-35.
- Preisinger, C., B. Short, V. De Corte, E. Bruyneel, A. Haas, R. Kopajtich, J. Gettemans, and F.A. Barr. 2004. YSK1 is activated by the Golgi matrix protein GM130 and plays a role in cell migration through its substrate 14-3-3zeta. *J Cell Biol.* 164:1009-1020.
- Raeis-Dauve, V., P. Philip-Couderc, G. Faggian, M. Tessari, A. Roatti, A.D. Milano, M.L. Bochaton-Piallat, and A.J. Baertschi. 2012. Increased expression of adenosine triphosphate-sensitive K⁺ channels in mitral dysfunction: mechanically stimulated transcription and hypoxia-induced protein stability? *J Am Coll Cardiol.* 59:390-396.
- Rajan, S., R. Preisig-Muller, E. Wischmeyer, R. Nehring, P.J. Hanley, V. Renigunta, B. Musset, G. Schlichthorl, C. Derst, A. Karschin, and J. Daut. 2002. Interaction with 14-3-3 proteins promotes functional expression of the potassium channels TASK-1 and TASK-3. *J Physiol.* 545:13-26.
- Rohrer, D.K., K.H. Desai, J.R. Jasper, M.E. Stevens, D.P. Regula, Jr., G.S. Barsh, D. Bernstein, and B.K. Kobilka. 1996. Targeted disruption of the mouse beta1-adrenergic receptor gene: developmental and cardiovascular effects. *Proc Natl Acad Sci U S A.* 93:7375-7380.
- Sahlmuller, M.C., J.R. Strating, R. Beck, P. Eckert, V. Popoff, M. Haag, A. Hellwig, I. Berger, B. Brugger, and F.T. Wieland. 2011. Recombinant heptameric coatomer complexes: novel tools to study isoform-specific functions. *Traffic.* 12:682-692.
- Schramm, T.K., G.H. Gislason, A. Vaag, J.N. Rasmussen, F. Folke, M.L. Hansen, E.L. Fosbol, L. Kober, M.L. Norgaard, M. Madsen, P.R. Hansen, and C. Torp-Pedersen. 2011. Mortality and cardiovascular risk associated with different

- insulin secretagogues compared with metformin in type 2 diabetes, with or without a previous myocardial infarction: a nationwide study. *European heart journal*. 32:1900-1908.
- Shen, C., M.J. Lin, A. Yaradanakul, V. Lariccia, J.A. Hill, and D.W. Hilgemann. 2007. Dual control of cardiac Na⁺ Ca²⁺ exchange by PIP(2): analysis of the surface membrane fraction by extracellular cysteine PEGylation. *J Physiol*. 582:1011-1026.
- Shikano, S., B. Coblitz, H. Sun, and M. Li. 2005. Genetic isolation of transport signals directing cell surface expression. *Nature cell biology*. 7:985-992.
- Shiota, C., O. Larsson, K.D. Shelton, M. Shiota, A.M. Efanov, M. Hoy, J. Lindner, S. Kooptiwut, L. Juntti-Berggren, J. Gromada, P.O. Berggren, and M.A. Magnuson. 2002. Sulfonylurea receptor type 1 knock-out mice have intact feeding-stimulated insulin secretion despite marked impairment in their response to glucose. *J Biol Chem*. 277:37176-37183.
- Smith, A.J., J. Daut, and B. Schwappach. 2011. Membrane proteins as 14-3-3 clients in functional regulation and intracellular transport. *Physiology (Bethesda)*. 26:181-191.
- Stocker, P.J., and E.S. Bennett. 2006. Differential sialylation modulates voltage-gated Na⁺ channel gating throughout the developing myocardium. *J Gen Physiol*. 127:253-265.
- Suzuki, M., N. Sasaki, T. Miki, N. Sakamoto, Y. Ohmoto-Sekine, M. Tamagawa, S. Seino, E. Marban, and H. Nakaya. 2002. Role of sarcolemmal K(ATP) channels in cardioprotection against ischemia/reperfusion injury in mice. *J Clin Invest*. 109:509-516.
- Tokuyasu, K.T. 1973. A technique for ultracryotomy of cell suspensions and tissues. *J Cell Biol*. 57:551-565.
- Tucker, S.J., F.M. Gribble, C. Zhao, S. Trapp, and F.M. Ashcroft. 1997. Truncation of Kir6.2 produces ATP-sensitive K⁺ channels in the absence of the sulphonylurea receptor. *Nature*. 387:179-183.
- Waterman, M.J., E.S. Stavridi, J.L. Waterman, and T.D. Halazonetis. 1998. ATM-dependent activation of p53 involves dephosphorylation and association with 14-3-3 proteins. *Nat Genet*. 19:175-178.
- Yamada, S., G.C. Kane, A. Behfar, X.K. Liu, R.B. Dyer, R.S. Faustino, T. Miki, S. Seino, and A. Terzic. 2006. Protection conferred by myocardial ATP-sensitive K⁺ channels in pressure overload-induced congestive heart failure revealed in KCNJ11 Kir6.2-null mutant. *J Physiol*. 577:1053-1065.
- Yan, F.F., Y.W. Lin, C. MacMullen, A. Ganguly, C.A. Stanley, and S.L. Shyng. 2007. Congenital hyperinsulinism associated ABCC8 mutations that cause defective trafficking of ATP-sensitive K⁺ channels: identification and rescue. *Diabetes*. 56:2339-2348.
- Yuan, H., K. Michelsen, and B. Schwappach. 2003. 14-3-3 dimers probe the assembly status of multimeric membrane proteins. *Current biology : CB*. 13:638-646.
- Zerangue, N., M.J. Malan, S.R. Fried, P.F. Dazin, Y.N. Jan, L.Y. Jan, and B. Schwappach. 2001. Analysis of endoplasmic reticulum trafficking signals by combinatorial screening in mammalian cells. *Proc Natl Acad Sci U S A*. 98:2431-2436.
- Zerangue, N., B. Schwappach, Y.N. Jan, and L.Y. Jan. 1999. A new ER trafficking signal regulates the subunit stoichiometry of plasma membrane K(ATP) channels. *Neuron*. 22:537-548.

- Zhao, W., T.L. Chen, B.M. Vertel, and K.J. Colley. 2006. The CMP-sialic acid transporter is localized in the medial-trans Golgi and possesses two specific endoplasmic reticulum export motifs in its carboxyl-terminal cytoplasmic tail. *J Biol Chem.* 281:31106-31118.
- Zingman, L.V., D.M. Hodgson, P.H. Bast, G.C. Kane, C. Perez-Terzic, R.J. Gumina, D. Pucar, M. Bienengraeber, P.P. Dzeja, T. Miki, S. Seino, A.E. Alekseev, and A. Terzic. 2002. Kir6.2 is required for adaptation to stress. *Proc Natl Acad Sci U S A.* 99:13278-13283.
- Zuzarte, M., K. Heusser, V. Renigunta, G. Schlichthorl, S. Rinne, E. Wischmeyer, J. Daut, B. Schwappach, and R. Preisig-Muller. 2009. Intracellular traffic of the K⁺ channels TASK-1 and TASK-3: role of N- and C-terminal sorting signals and interaction with 14-3-3 proteins. *J Physiol.* 587:929-952.

FIGURE LEGENDS

Fig. 1 Biochemical analysis of K_{ATP} channel subunits in atria and ventricles. (A) Western blot (see Table S1 for antibodies) for SUR2A, SUR1, Kir6.2 and $\alpha 1$ subunit of the Na,K-ATPase ‘Na,K’ in membranes from mouse atrial ‘A’ and ventricular tissue ‘V’. Filled arrowhead and asterisks indicates core- and complex-glycosylated SURs, respectively. Blot is representative of three independent experiments. (B) Confocal analysis of immunostained mouse ventricular myocytes ‘VM’. Anti-SUR2A (red) and anti-Kir6.2 (green) signals are shown by region of interest (ROI) indicated in merged whole cell image (dashed white box). Kir6.2 nuclear staining is unspecific (see Fig. S2 for knockout control). PDM denotes product of differences from the mean indicating co-localization by intensity correlation analysis (Li et al., 2004). Values of intensity correlation quotient between 0 and 0.5 indicate codependent staining and were 0.16 ± 0.005 for VM (n=11). Scale bars 10 μ m. (C) Schematic representation of SUR1 and Kir6.2 as cargo proteins of the early secretory pathway and rationale of glycan analysis using endoglycosidase H and PNGase F. Shapes and symbols are identified by boxed key. (D) Western blot for SUR1, Kir6.2 and Na,K in membranes from mouse atrial ‘A’ and ventricular ‘V’ tissue. Treatment with Endo H as indicated, open arrowhead, filled arrowhead, and asterisks mark deglycosylated, core-glycosylated, and complex-glycosylated forms of SUR1, respectively. Na,K serves as loading control. Blot is representative of six independent experiments. (E) Western blot for SUR1 in membranes from rat atrial ‘A’ and ventricular ‘V’ tissue demonstrating differential migration behaviors. Filled arrowhead indicates the core- and asterisks two complex-glycosylated forms of SUR1. The panel shows three technical replicates (proteins resolved on gels of increasing percentages – 6%, 7% and 8%) of two biological replicates (from two rats, ‘#1’ and ‘#2’). The blot is representative of eight independent experiments. (F) PNGase F glycosidase ‘PNG F’ treatment of solubilized membranes from rat atrial ‘A’ or ventricular ‘V’ tissue to probe whether differences in SUR1 migratory behavior (asterisks) were caused by differential complex glycosylation. Migration differences disappeared upon deglycosylation (indicated by open arrowhead). Filled arrowhead indicates the core- and asterisks the complex-glycosylated forms of SUR1. The blot is representative of eleven independent experiments.

Fig. 2 SUR1/Kir6.2 K_{ATP} channels are differentially localized in atrial and ventricular myocytes. (A) Confocal analysis of immunostained mouse atrial ‘AM’ or ventricular ‘VM’ myocytes. Anti-SUR1 (red) and anti-Kir6.2 (green) immunofluorescence signals are shown by ROI as indicated in the whole cell image (‘merge’, dashed white box). Values of intensity correlation quotient (ICQ): AM 0.20 ± 0.007 S.E.M (n=7) and VM 0.14 ± 0.008 S.E.M (n=4) confirming co-localization of Kir6.2/SUR1 subunits. Scale bars 10 μ m. Refer to Fig. 8 for orientation on cardiac myocyte morphology. (B) Cell surface PEGylation analysis in intact mouse hearts (Shen et al., 2007) indicating cell surface expression of SUR1 in atrial but not in ventricular myocytes. Modified bands are marked by a ‘C’; sodium calcium exchanger (NCX) is shown as positive control for cell surface PEGylation. Kir6.2 and Na,K are not PEGylated and serve as negative controls. Blot is representative of three independent experiments quantified in (C). Note that the PEG modification is sensitive to reducing agents. Hence, non-reducing conditions were employed in contrast to all other Figures. Therefore, the core- and complex-glycosylated forms of SUR1 were not resolved. (C) Bar graph depicts the ratio of intensity of the labeled, PEGylated SUR1 species (‘C’ in Fig. 2B) and unlabeled SUR1 (black arrowhead in Fig. 2B) for atria (open bars) and ventricles (filled bars). Increased PEGylation in atria was statistically significant ($p < 0.05$) whereas the PEGylated species was not significantly increased in ventricular membranes. (D) PEGylation of epitope-tagged SUR1-4PC and Kir6.2 in HEK293 cells. Western blot against the PC-epitope is shown for PEG-maleimide treated sample and untreated control. ‘C’ indicates position of PEGylated SUR1 species. (E) SUR1 is only PEGylated upon co-expression with Kir6.2 or when the Arg-based retrieval signal is inactivated by site-directed mutagenesis (SUR1-4PC_{AAA}) consistent with Arg-based retrieval signals preventing unassembled subunits from reaching the cell surface.

Fig. 3 SUR1/Kir6.2 K_{ATP} channels are retained in the Golgi of ventricular myocytes. (A) PNGase F glycosidase ‘PNG F’ treatment of solubilized membranes from rat atrial ‘A’ or ventricular ‘V’ tissue. Like SUR1, the sodium channel α -subunit Nav1.5 displayed differential migratory behavior (asterisks) between atria and ventricles whereas β -adrenergic receptor ‘ β 1-AR’ and β -dystroglycan ‘ β -DG’ migration was indistinguishable in the two tissues. Na,K is not glycosylated and serves as loading

control. All three glycoproteins were fully deglycosylated by PNGase F (open arrowhead) leading to loss of differential migration. The blot is representative of three independent experiments. (B) Confocal analysis of immunostained mouse atrial ‘AM’ or ventricular ‘VM’ myocytes. Anti-SUR1 (red) and anti-p115 (green) immunofluorescence signals are shown by ROI in the whole cell image (‘merge’, dashed white box). For ‘PDM’ (product of differences from the mean) analysis see Fig. 1. Scale bars 10 μ m. Refer to Fig. 8 for orientation on cardiac myocyte morphology. (C) Treatment of rat atrial and ventricular membranes with neuraminidase as indicated to probe extent of sialylation of SUR1. Blot is representative of five independent experiments. (D) SDS eluates from wheat germ agglutinin column (WGA) probed with indicated antibodies. Asterisks indicate differential migration of Nav1.5 and SUR1. The blot is representative of three independent experiments. (E) Silver-stained eluates from WGA. Asterisk indicates one prominent differential band identified as peptidylglycine α -amidating monooxygenase. (C,D,E: rat cardiac tissue).

Fig. 4 β -adrenergic stimulation deploys Golgi-stalled SUR1/Kir6.2 channels to T-tubule membrane invaginations at striations of ventricular myocytes. (A) Confocal analysis of mouse ventricular myocytes immunostained for SUR1 in absence or presence of 10 μ M isoproterenol ‘ISO’ and 10 μ M rolipram ‘ROL’. Dashed boxes indicate the magnified (2x) intracellular region of interest (middle) and the binary inverse contrasted signal (bottom). Scale bar 10 μ m. Refer to Fig. 8 for orientation on cardiac myocyte morphology. (B) Power spectrum (Fourier analysis) of 20 untreated versus 18 treated myocytes; the 1st peak indicates the degree of periodicity of the striated signal (arrowhead). (C) Bar graph summarizing average change in power at the 1st peak marked in (B); error bars show standard error of the mean (S.E.M). (D) Inside-out patch clamp recordings of mouse ventricular myocytes untreated or treated for one hour and during recordings. ‘Relative current’ refers to the fraction of current in zero ATP that is activated by diazoxide or pinacidil. Bar graphs represent 16 to 17 cells, error bars reflect S.E.M. and individual data points are shown as circles (untreated) or squares (treated). Three stars indicate significance $p < 0.0005$. (E) Inside-out patch clamp recordings of mouse ventricular myocytes untreated or treated with 10 μ M isoproterenol and 10 μ M rolipram each for one hour and during

recordings. I_{max}, is the maximum current in zero ATP. (F) Western blot for SUR1, Na,K, Kir6.2 and the phosphorylated form of phospholamban (phosphoserine S16) in membranes and 14-3-3 proteins and GAPDH in cytosol from mouse ventricular myocytes untreated or treated as in (A)-(E). The blot is representative of three independent experiments

Fig. 5 Ventricular myocytes contain significantly lower amounts of 14-3-3. Western blot (A) and quantification (B) of three independent experiments using a pan-reactive 14-3-3 antibody cocktail (Table S1-antibodies 1b and 1c). Indicated amounts of soluble cellular lysate from rat atrial 'AM' or ventricular 'VM' myocytes were loaded. Varying concentrations of recombinant 14-3-3 β were used to approximate detection threshold of the pan-reactive antibody. Glyceraldehyde-3-phosphate dehydrogenase (GAPDH) was detected as loading control. (C) Confocal analysis of immunostained mouse atrial 'AM' or ventricular 'VM' myocytes. Anti-14-3-3 (red) and anti-p115 (green) immunofluorescence signals are shown by ROI indicated in whole cell image ('merge', dashed white box). Scale bars 10 μ m. Refer to Fig. 8 for orientation on cardiac myocyte morphology. (D) Two different examples of immunoelectron microscopy performed on fixed cryosections from mouse left ventricle. Upper picture indicates inset shown in lower panel. I, M and Z indicate the respective bands of the cardiac muscle. Mi, mitochondria and arrows point to the gold label (14-3-3: 6 nm and p115: 10 nm). Scale bars: black 500 nm; white 200 nm (boxed inset magnification). (E) RT-PCR analysis of six 14-3-3 isoforms using mRNA from isolated rat atrial 'AM' and ventricular 'VM' myocytes. mRNA abundance is normalized to the message encoding GAPDH. Bar graphs summarize three biological replicates. One asterisk denotes $p < 0.05$, two $p < 0.01$, non-significant value of $p < 0.07$ is indicated for two isoforms.

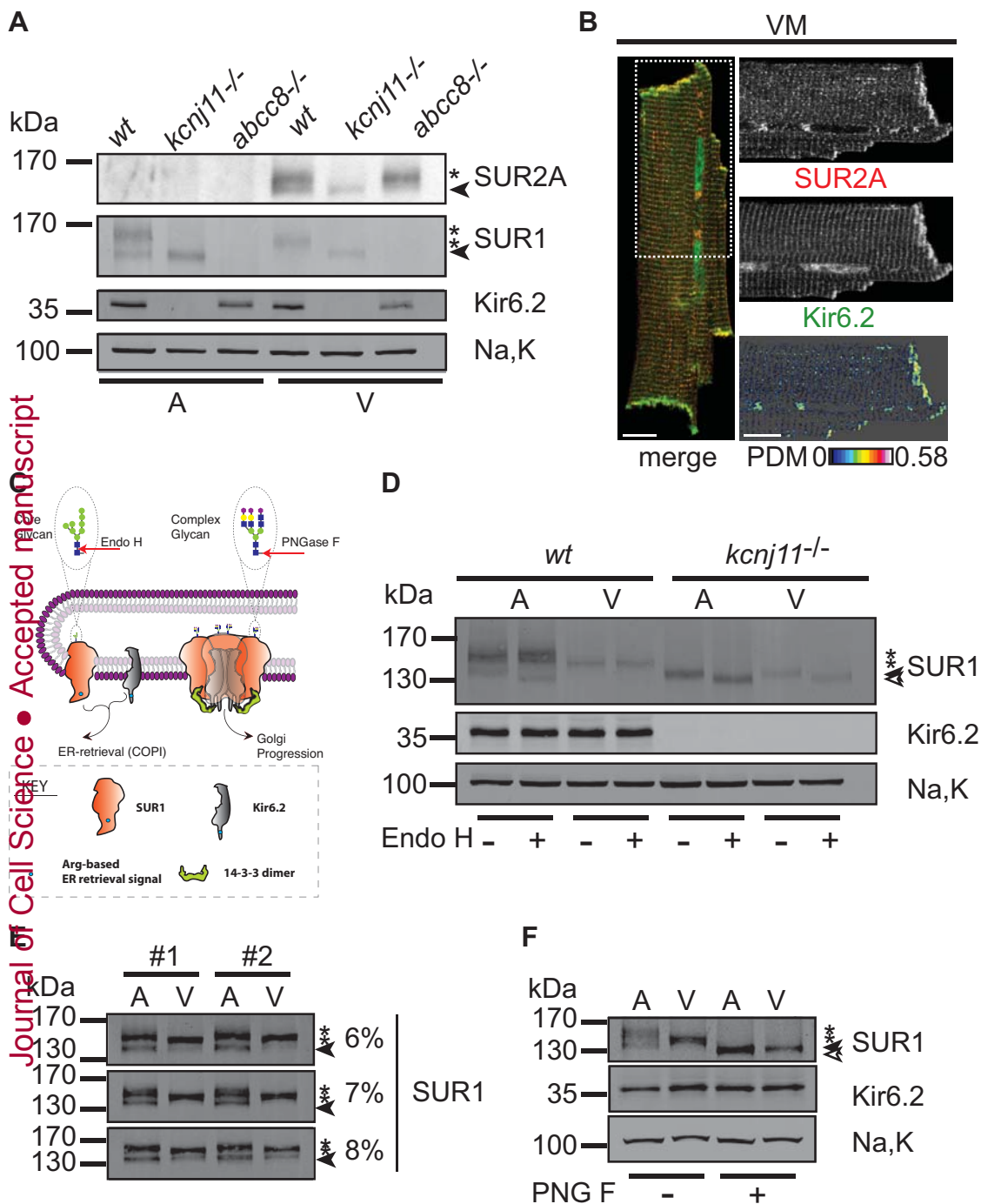
Fig. 6 Phosphorylation of the Kir6.2 C-terminus by PKA reduces COPI and 14-3-3 binding. (A) Western blot for Kir6.2, Phospholamban (PLN), a phosphorylated form of phospholamban (phosphoserine 16) and substrates phosphorylated by PKA (PKA pSub Ab) in hearts perfused in the presence (+) or absence (-) of 10 μ M isoproterenol and 10 μ M rolipram. (B) Phosphorylated Kir6.2 was immunoprecipitated using an antibody (PKA pSub Ab) that binds PKA phosphorylated substrates. Solubilized

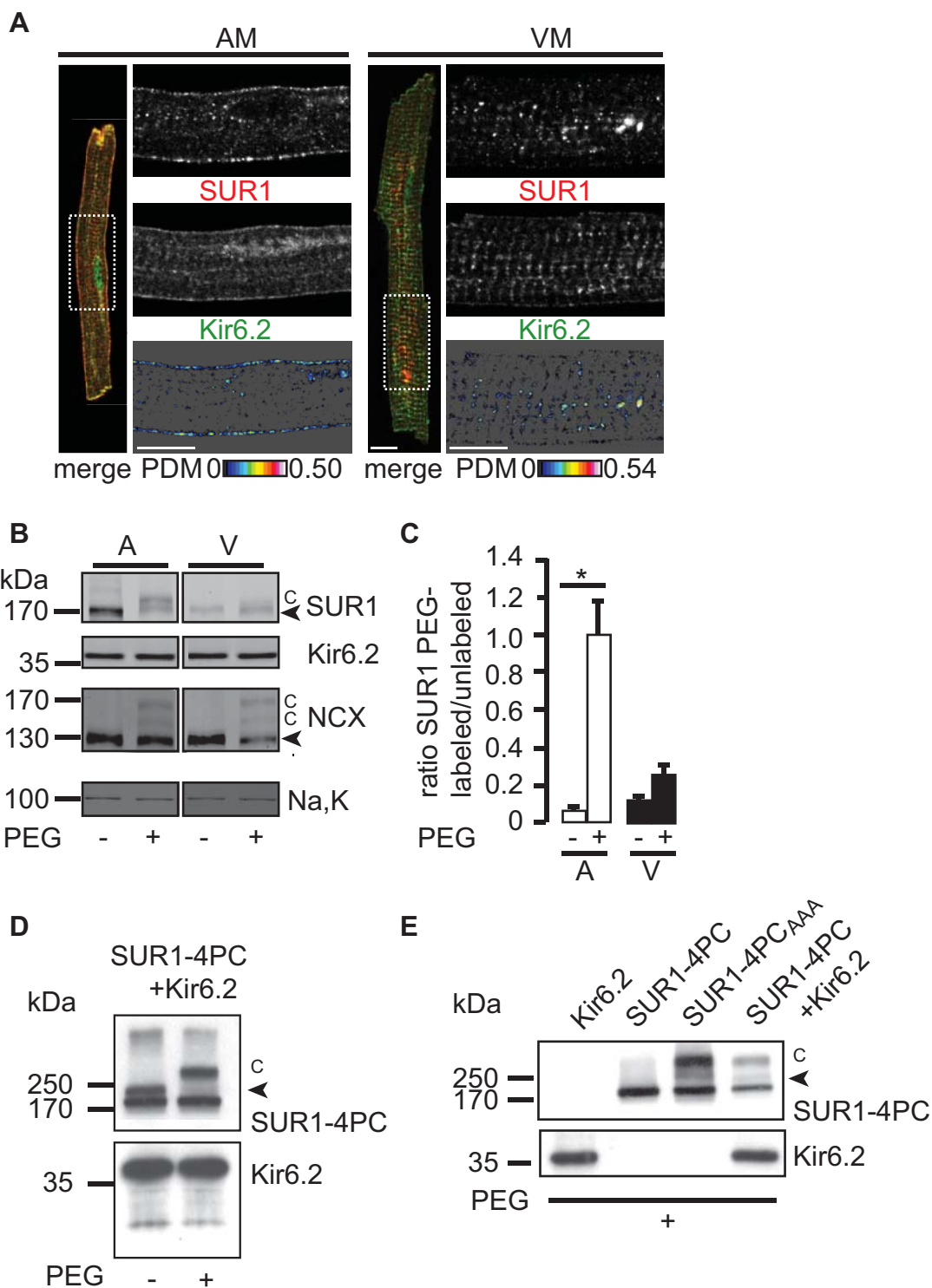
membranes prepared from treated (+) or untreated (-) hearts as in (A) were used. The blots were probed for Kir6.2 (IB, immunoblot). Purified Rabbit IgG was used as a negative control. IgG LC refers to the antibody light chain and serves as a loading control. (C) COPI binding assay reveals reduction of COPI binding after phosphorylation of the C-terminus of Kir6.2. Compare Fig. S4 for the quantification of three independent experiments. (D) 14-3-3 binding assay reveals reduction of 14-3-3 binding after phosphorylation of the C-terminus of Kir6.2. The gel is representative of three independent experiments. (E) Model depicting release of SUR1-containing K_{ATP} channels from the antagonistic action of COPI and 14-3-3 after phosphorylation.

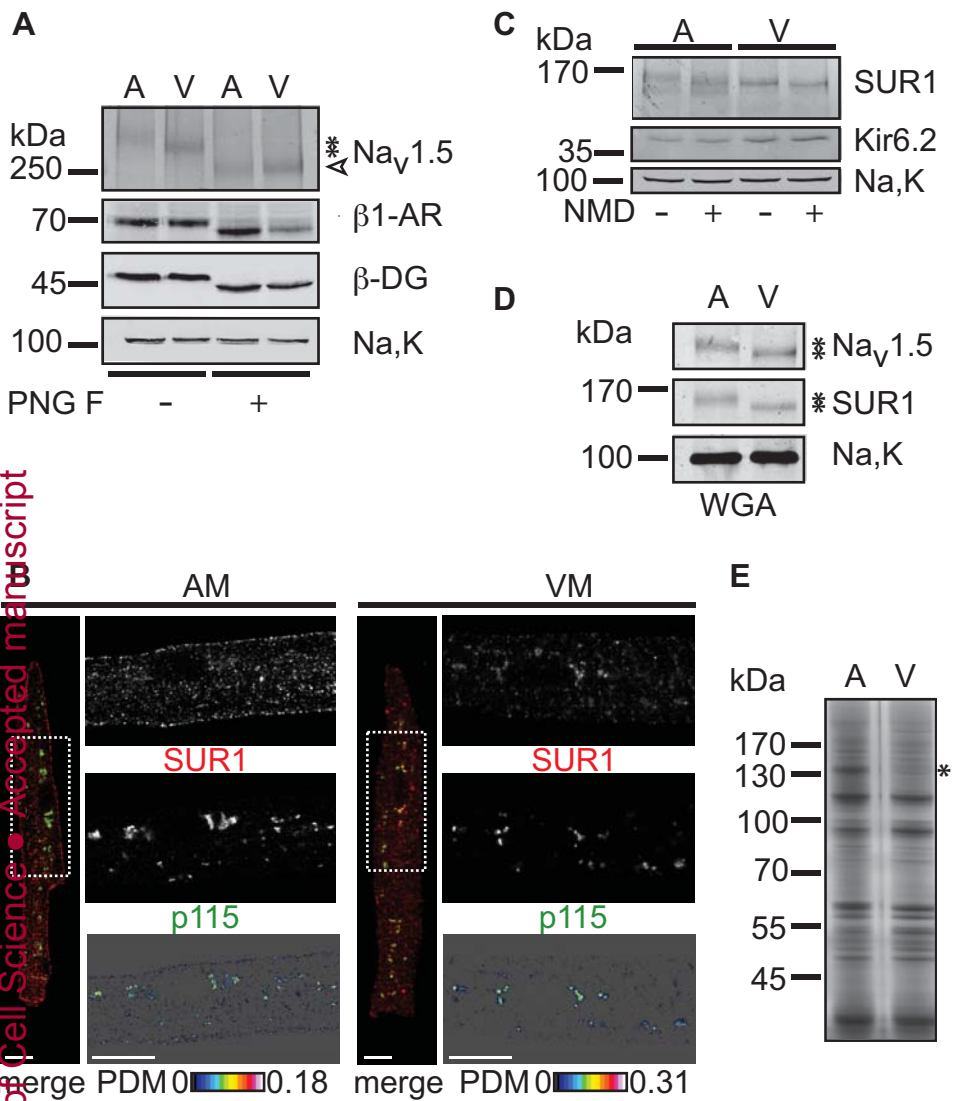
Fig. 7 Action potential shortening during sustained β -adrenergic stimulation requires SUR1. (A) Representative APD maps from a WT (top) and *abcc8*^{-/-} (bottom) ventricle were constructed from optical mapping recordings during control (left), 20 minutes after 10 μ M ISO/10 μ M ROL (center) administration, and 10 minutes after addition of 10 μ M Glibenclamide (right). Each pixel in the map represents APD80 from that region of the ventricular myocardium according to the colorbar on the left. (B) Signal averaged action potential traces from representative WT and *abcc8*^{-/-} ventricles are shown. (C) Normalized APD from WT hearts (n=5) shows significant shortening (at 80% repolarization) in ISO/ROL and clear reversal with Glibenclamide. However, normalized APD from *abcc8*^{-/-} hearts (n=5) show no significant changes throughout the experiment.

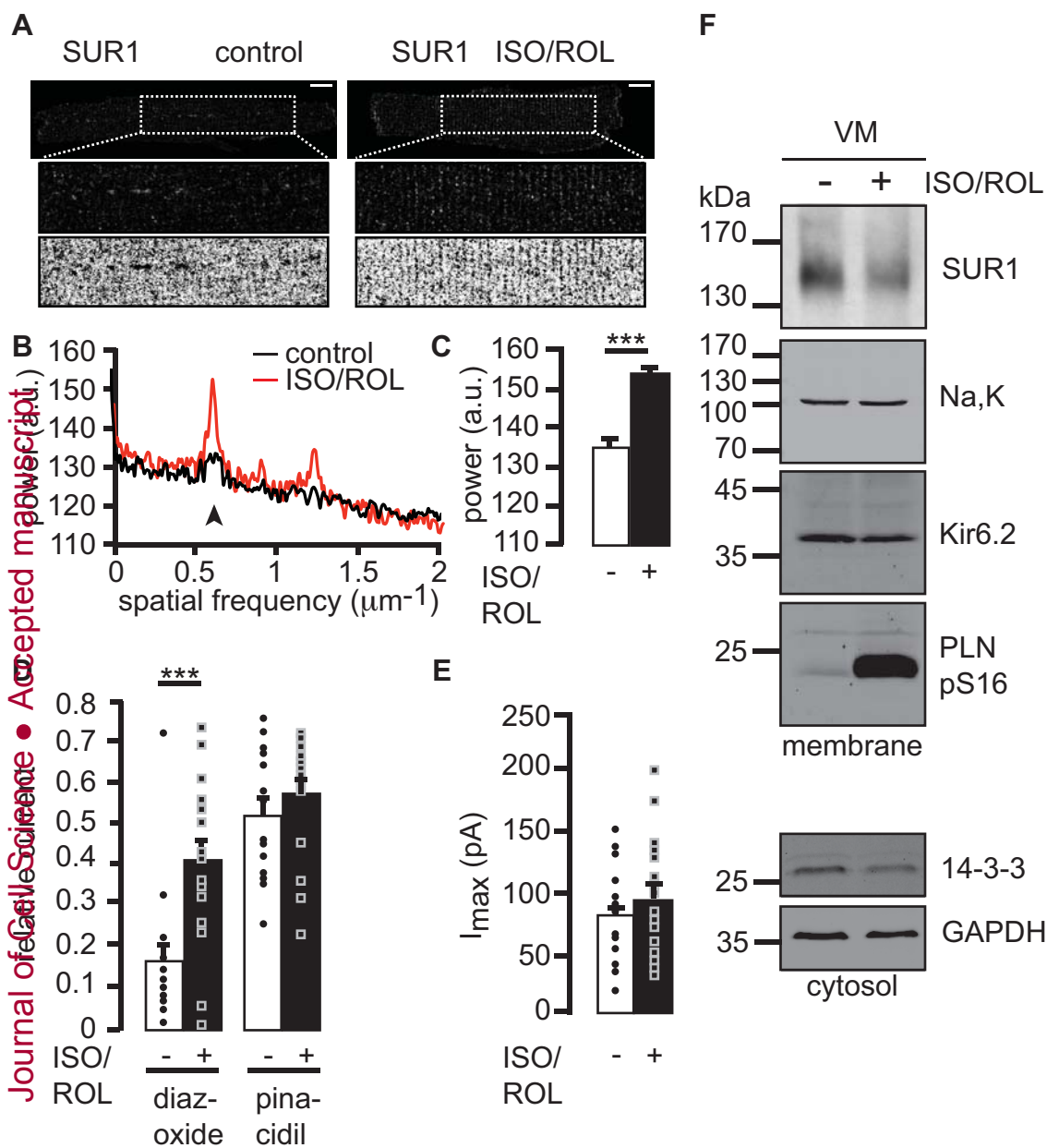
Fig. 8 Model of the regulated deployment of SUR1/Kir6.2 K_{ATP} channels in ventricular myocytes. (A) Agonist (Isoproterenol) binding to beta-adrenergic receptors (β -AR) triggers the activation of the adenylyl cyclase (AC) via a β -AR coupled G-protein, resulting in elevation of cAMP and activation of PKA. Attenuation of signal transduction via degradation of cAMP by phosphodiesterase (PDE), was inhibited using the PDE4 specific inhibitor rolipram. Known PKA targets include the voltage-gated calcium channel (Cav1.2) and the Ryanodine receptor (RyR2), culminating in elevation of cytosolic Ca^{2+} (by release from the sarcoplasmic reticulum (SR) Ca^{2+} stores and by influx of extracellular Ca^{2+}). Phosphorylation of phospholamban (PLN) by PKA relieves its inhibitory effect on the SR calcium pump (SERCA). For the sake of simplicity, the relevant PKA holoenzyme has been depicted

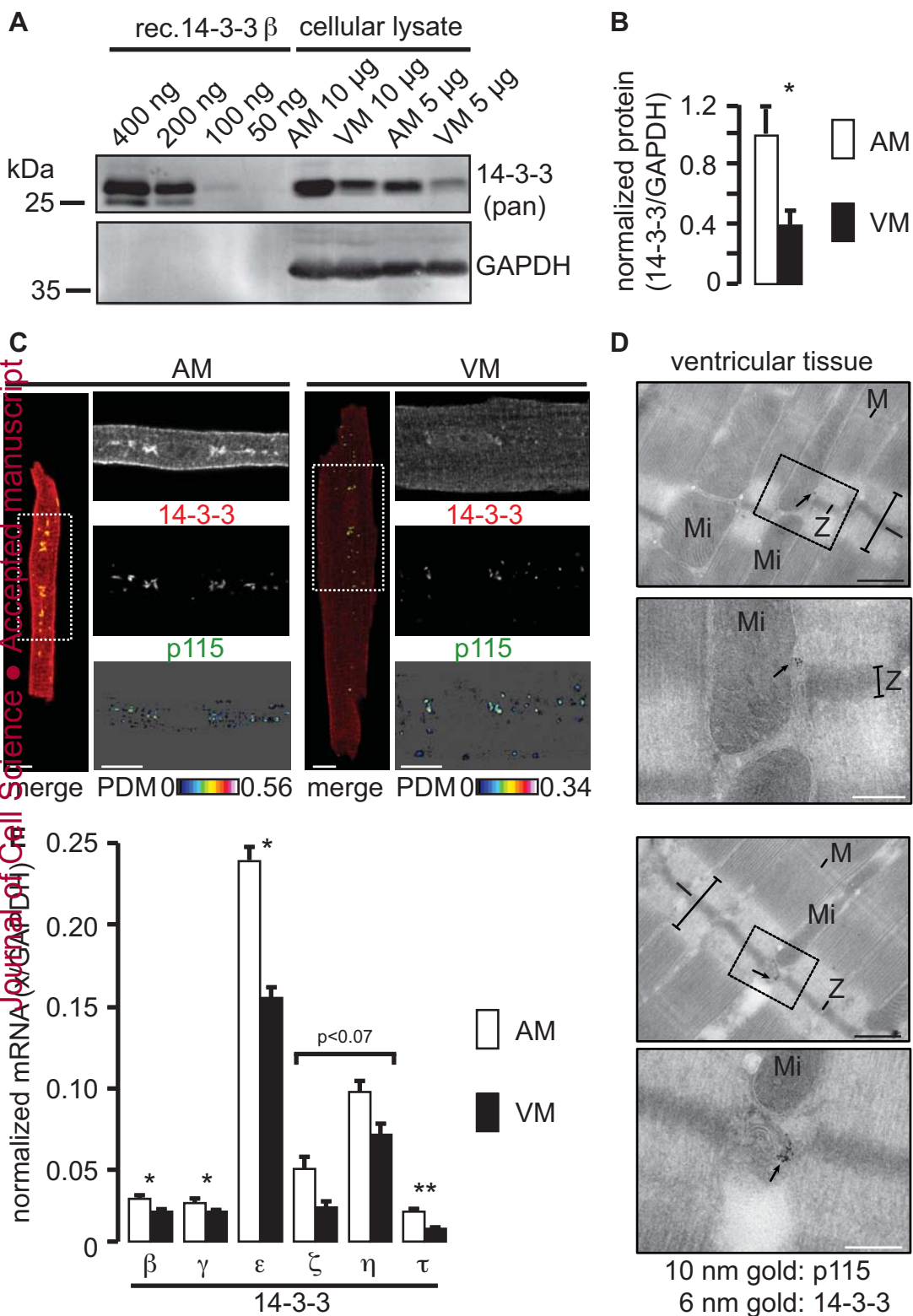
as being cytosolic and not membrane associated. (B) PKA dependent phosphorylation of S372 (adjacent to the Arg-based ER retrieval signal) in Kir6.2 releases Golgi-stored SUR1/Kir6.2 K_{ATP} channels from COPI binding thus facilitating Golgi exit. An unknown kinase anchoring protein (AKAP) conceivably localizes PKA to the vicinity of K_{ATP} channels. (C) Deployment of SUR1-containing K_{ATP} channels from the Golgi to the T-tubular plasma membrane. Hypothetically, signal transduction may affect the available pool of 14-3-3 proteins, in addition to direct phosphorylation of cargo proteins by shifting the equilibrium between an engaged (substrate bound) and available (substrate free) pool, thus overcoming the limitations of cell surface expression of 14-3-3 substrates by the limited availability of 14-3-3 proteins.











Science • Accepted manuscript
 Cell (www.sciencemag.org)

